# Subspace-Based and DIRECT Algorithms for Distorted Circular Contour Estimation

Julien Marot and Salah Bourennane

***Abstract*—Circular features are commonly sought in digital image processing. The subspace-based line detection (SLIDE) method proposed to estimate the center and the radius of a single circle. In this paper, we introduce a novel method for estimating several radii while extending the circle estimation to retrieve circular-like distorted contours. Particularly, we develop and validate a new model for virtual signal generation by simulating a circular antenna. The circle center is estimated by the SLIDE method. A variable speed propagation scheme toward the circular antenna yields a linear phase signal. Therefore, a high-resolution method provides the radius. Either the gradient method or the more robust combination of dividing rectangles and spline interpolation can extend this method extend this method for free form object segmentation. The retrieval of multiple non concentric circles and rotated ellipses is also considered. To evaluate the performance of the proposed methods, we compare them with a least-squares method, Hough transform, and gradient vector flow. We apply the proposed method to hand-made images while considering some real-world images.**

***Index Terms*—Array processing, circular antenna, contour, image, optimization.**

## I. Introduction

CIRCULAR features are commonly sought in digital image processing. Circle fitting is suitable in several domains such as quality inspection for food industry, mechanical parts [1], and particle trajectories [2], [3]. Circle fitting has been applied in microwave engineering [4] and ball detection for robotic vision systems [5]. Nearly circular features are sought in character recognition; [6] and [7] proposed a template-based system for online character recognition, where the representative templates are automatically counted. These templates are viewed as different writing styles for any character. Ordinary or total least-squares methods for circle fitting seek to minimize the squares sum of error-of-fit with respect to measures [8]–[11]. Using geometric fitting [8], error distances are defined with the orthogonal, or shortest, distances from given points to the geometric feature to be fitted. In [10], a least-squares fitting approach is proposed. It is based on the hypothesis that a set of circular arcs extracted from the image is related to a set of circles contained in a model by translation, rotation and scaling. [10] presents an analytical solution based on least-squares fitting to obtain an optimal geometric transformation for the alignment of the circular arcs with circles. For a single circular arc, this method is easy to implement. For multiple arcs with different centers, this method relies on the strong hypothesis that all model circles should be transformed by the same translation, rotation, and scaling operations to fit the arcs in the image. One of the major limitations of most of least-squares approaches is their sensitivity to outliers [10]; [12] and [13] focused on planar spline interpolation between control-points by quadratic rational Bézier curves, to retrieve circular arcs. Compared to [10], this method does not take into account the prior knowledge of models or templates. It is based on interpolation between control-points. Other methods support circle retrieval, even in a noisy environment. The generalized Hough transform (GHT) provides estimation of the circle center coordinates when their radius is known [14], [15]. Its main drawback is the computational load, although fast versions have been proposed [16]. Contour-based snakes methods [17], such as the gradient vector flow (GVF), were largely used [18], [19] to retrieve concavities and weak edges with blurred boundaries. GVF limitations can be observed when the expected contour exhibit a high curvature. Levelset type methods [20], [21] enhance blindly all contours in images. Levelset does not provide explicitly the characteristics of contours with particular predefined parameters. Array processing methods [22], [23] have been proposed to find some characteristics of circular contours. The formalism proposed by Aghajan [22] detects circular or elliptic contours. A propagation phenomenon and the impinging of a wavefront upon the antenna are simulated through a variable speed propagation scheme. The center vertical and horizontal coordinates are estimated by placing the antenna successively at the top and left sides of the image; [22] proposed a radius estimation method, which relies on an approximation. This method can obtain a subimage from the initial image in such a way the top left corner is centered on the circle center, that was previously estimated. In [22], Aghajan showed that a truncation of the Taylor series of the generated signal leads to the value of the radius of the expected circle.

In this paper, we propose a new approach for radius estimation, and for the retrieval of distortion between any nearly circular contour and a circle. The approach uses a circular antenna. Particularly, we adapt an optimization method to retrieve a nearly circular contour. We consider concentric and non concentric features, either nearly circular or nearly oval. In [24] and [25], we adopted a similar strategy for approximately rectilinear distorted contours. In [24] and [25], a uniform linear array was used. It was demonstrated that array processing methods applied to contour detection are robust to noise impairment and

Manuscript received July 18, 2006; revised June 8, 2007. The associate editor coordinating the review of this manuscript and approving it for publication was Dr. Gaudenz Danuser.

The authors are with the Institut Fresnel/CNRS UMR 6133-Domaine Universitaire de Saint Jérôme F-13397 Marseille Cedex 20, France (e-mail: julien.marot@fresnel.fr; salah.bourennane@fresnel.fr).

Color versions of one or more of the figures in this paper are available online at http://ieeexplore.ieee.org.

Digital Object Identifier 10.1109/TIP.2007.903907

yield fast algorithms. As it will be illustrated later, the proposed approach based on circular antenna exhibits the same robustness and speed properties. Another advantage of the proposed method over the Hough transform method is that the estimates in our approach are inherently continuous, whereas in the Hough transform method, the resolution is limited by the bin size chosen for the parameter research interval. The proposed optimization approach retrieves any pixel shift value, whatever the curvature of the contour.

The remainder of the paper is organized as follows. In Section II, the problem of circle retrieval is highlighted, while explaining how to generate a signal from the image, upon a circular antenna. In Section III, a signal model is derived. We will show that a linear phase signal is obtained when circles are expected and either variable [26] or constant propagation parameter is adopted for signal generation. By using the minimum description length (MDL) criterion [23], [27], the number of concentric features is detected; then a high-resolution method [28] estimates the possibly close radius values of the expected concentric circles. Then, the proposed approach is generalized to retrieving several circles or ellipses with different centers and radii. In Section IV, the retrieval of circular contours is extended to any closed contour fitted by a circle. Optimization methods are investigated for this purpose. The fast variable step gradient method and the robust dividing rectangles (DIRECT) method [29] are accelerated using spline interpolation. In Section V, we discuss the results obtained by the proposed approach when it is applied to hand-made and real-world images. The proposed radius estimation method is compared with least-squares fitting and Hough transform applied to radius estimation [16]. Our optimization method is compared with GVF [18], in particular, concerning the robustness to noise and contour curvature.

## II. Problem Statement and Signal Generation

### A. Problem Statement

We highlight the problem of radius estimation, and the distortions between a closed contour and a circle that fits with this contour. We propose a circular antenna that enables a particular signal generation. We emphasize the phase of the generated signals. The generated signals fit classical array processing and optimization methods, contrary to signals derived by the existing signal generation methods [22]. Fig. 1(a) presents a binary digital image $I$ as a square matrix of dimensions $N \times N$. Each element represents an image pixel. An object in the image is made of edge pixels with value 1, over a background of zero-valued pixels. The object is fitted by a circle with radius value $r$ and center coordinates $(l_c, m_c)$. Fig. 1(b) shows a subimage extracted from the original image so that its top left corner is the center of the circle. This subimage is associated with a set of polar coordinates $(\rho, \theta)$. Each pixel of the expected contour in the subimage has the following coordinates: $r + \Delta\rho$, $\theta$. $\Delta\rho$ is the shift between the contour pixel and the circle one that fits the contour and which has the same coordinate $\theta$. We seek for star-shaped contours, that is, contours described by the relation $\rho = f(\theta)$, where $f$ is any function that maps $[0, 2\pi]$ to $\mathbb{R}_+$.

A traditional circle fitting method is the generalized Hough transform (GHT) [15], [16]. We employ a variant of Hough transform that estimates the radii of concentric circles when their center is known. Its basis is to count the number of pixels which are located on a circle for all possible radius values. The drawback of Hough transform is its elevated computational load. From this emerges the need for a faster radius estimation. In [22], [23], and [30], Aghajan *et al.* replaced the Hough transform by the much faster subspace-based line detection (SLIDE) algorithm to retrieve straight lines. Existing algorithms [24], [25] adapt an optimization method to signals generated upon a linear antenna composed of one sensor per row. When the expected contours consist of one pixel per row, only one unknown parameter of the optimization problem is included in one component of the generated signal [24], [25].

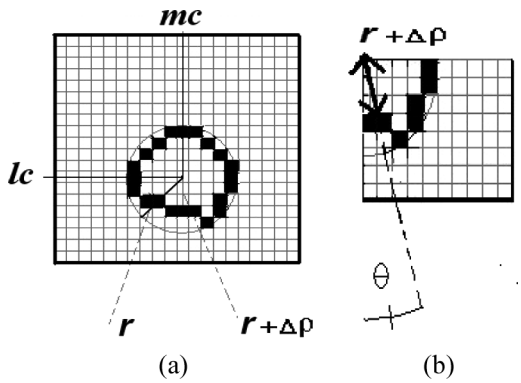


Fig. 1. (a) Circular-like contour. (b) Bottom right quarter of the contour and pixel coordinates in the polar system $(\rho, \theta)$ having its origin on the center of the circle. $r$ is the radius of the circle. $\Delta\rho$ is the value of the shift between a pixel of the contour and the pixel of the circle having same coordinate $\theta$.

Contours which are approximately circular are supposed to be made of more than one pixel per row for some of the rows of the image and more than one pixel per column for some columns of the image. Several pixels may lead to only one signal component. A linear antenna does not lead to a linear phase signal when a circular contour is present in the image.

### B. Virtual Signal Generation

We set an analogy between the estimation of a circular contour in an image and the estimation of a wavefront in array processing. The basic idea is to obtain a linear phase signal from an image containing a quarter of circle. To achieve this, we use a circular antenna. The phase of the signals which are virtually generated on the antenna is constant or varies linearly as a function of the sensor index. A quarter circle with radius $r$ and a circular antenna are represented in Fig. 2. The antenna is a quarter of circle centered on the top left corner, and crossing the bottom right corner of the subimage. Such an antenna is adapted to the subimages containing each quarter of the expected contour (see Fig. 2). In practice, the extracted subimage is possibly rotated so that its top left corner is the estimated center. The antenna has radius $R_a$ so that $R_a = \sqrt{2}N_s$ where $N_s$ is the number of rows or columns in the subimage. When we consider the subimage which includes the right bottom part of the expected contour, the following relation holds: $N_s = \max(N - l_c, N - m_c)$ where $l_c$ and $m_c$ are the vertical and horizontal coordinates of the center of the expected contour in a cartesian set centered on the top left corner of the whole processed image (see Fig. 1). Coordinates

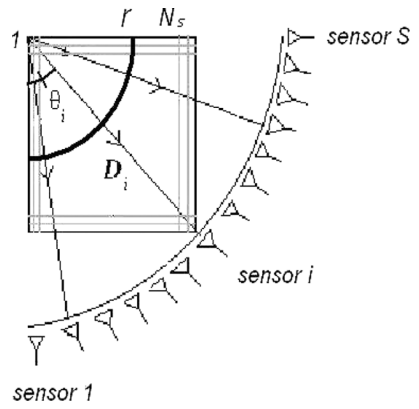


Fig. 2. Subimage, associated with a circular array composed of S sensors.

$l_c$ and $m_c$ are estimated by the method proposed in [22], or the one that is detailed later in this paper.

Signal generation scheme upon a circular antenna is the following: the directions adopted for signal generation are from the top left corner of the subimage to the corresponding sensor. The antenna is composed of S sensors, so there are S signal components.

Let us consider $D_i$, the line that makes an angle $\theta_i$ with the vertical axis and crosses the top left corner of the subimage. The $i$th component $(i = 1, \ldots, S)$ of the signal $\mathbf{z}$ generated out of the image reads

$$z(i) = \sum_{\substack{l,m=1 \\ (l,m)\in D_i}}^{l,m=N_s} I(l,m)\exp(-j\mu\sqrt{l^2+m^2}). \qquad (1)$$

The integer $l$ (resp., $m$) indexes the lines (resp., the columns) of the image. $j$ stands for $\sqrt{-1}$. $\mu$ is the propagation parameter [26]. Each sensor indexed by $i$ is associated with a line $D_i$ having an orientation $\theta_i = ((i-1)\cdot\pi/2)/S$. In (1), the term $(l,m) \in D_i$ means that only the image pixels that belong to $D_i$ are considered for the generation of the $i$th signal component. Satisfying the constraint $(l,m) \in D_i$, that is, choosing the pixels that belong to the line with orientation $\theta_i$, is done in two steps: let $setl$ be the set of indexes along the vertical axis, and $setm$ the set of indexes along the horizontal axis. If $\theta_i$ is less than or equal to $\pi/4$, $setl = [1 : N_s]$ and $setm = \lfloor [1 : N_s] \cdot \tan(\theta_i) \rfloor$. if $\theta_i$ is greater than $\pi/4$, $setm = [1 : N_s]$ and $setl = \lfloor [1 : N_s] \cdot \tan(\pi/2 - \theta_i) \rfloor$. Symbol $\lfloor \cdot \rfloor$ means integer part. The minimum number of sensors that permits a perfect characterization of any possibly distorted contour is the number of pixels that would be virtually aligned on a circle quarter having radius $\sqrt{2}N_s$. Therefore, the minimum number $S$ of sensors is $\sqrt{2}N_s$.

## III. Proposed Method for Radius and Center Estimation

*Estimation of Multiple Concentric Circles:* Most often, there exists more than one circle for one center. We demonstrate how several possibly close radius values can be estimated using a high-resolution method. We propose an estimation method for the number $d$ of concentric circles, and each radius value. For this purpose, we employ a variable speed propagation scheme [26]. We set $\mu = \alpha(i-1)$, for each sensor indexed by $i = 1, \ldots, S$. From (1), the signal received on each sensor is

$$z(i) = \sum_{k=1}^{d} \exp(-j\alpha(i-1)r_k) + n(i), \quad i = 1, \ldots, S \qquad (2)$$

where $r_k$, $k = 1, \ldots, d$ are the values of the radius of each circle, and $n(i)$ is a noise term due to outliers. All components $z(i)$ compose the observation vector $\mathbf{z}$. Total least-squares-estimation of parameters by rotational invariance techniques (TLS-ESPRIT) algorithm requires the estimation of the covariance matrix of several snapshots. There is no time-dependent signals. So, the question arises as to how a sample covariance matrix can be formed. This can be done as follows [23]. From the observation vector, we build $K$ subvectors of length $M$ with $d < M \leq S - d + 1$ : $\mathbf{z}_l = [z(l), \cdots, z(l+M-1)]^T$, $l = 1, \cdots, K$. To maximize the number of snapshots [24], the first component of a snapshot is the second component of the previous snapshot. This improves the estimation of the covariance matrix that is performed in TLS-ESPRIT algorithm. We then obtain $K = S + 1 - M$ snapshots. Grouping all subvectors obtained in matrix form, we get $\mathbf{Z}_K = [\mathbf{z}_1, \cdots, \mathbf{z}_K]$, where

$$\mathbf{z}_l = \mathbf{A}_M \mathbf{s} + \mathbf{n}_l, \quad l = 1, \cdots, K. \qquad (3)$$

$\mathbf{A}_M = [\mathbf{a}(r_1), \cdots, \mathbf{a}(r_d)]$ is a Vandermonde type matrix of size $M \times d$: the $i$th component of $\mathbf{a}(r_k)$ is $\exp(-j\alpha(i-1)r_k)$. $\mathbf{s}$ is a length $d$ vector equal to $[1, 1, \ldots, 1]^T$-superscript $^T$ denotes transpose- and $\mathbf{n}_l = [n(l), \cdots, n(l+M-1)]^T$.

The signal model of (3) suits TLS-ESPRIT method, a subspace-based method that requires the dimension of the signal subspace, that is, in this problem, the number of concentric circles. MDL criterion estimates the dimension of the signal subspace [23] from the eigenvalues of the covariance matrix. TLS-ESPRIT is applied on the measurements collected from two overlapping subarrays, and falls into two parts: the covariance matrix estimation and the minimization of a total-least-squares criterion. The radius values are obtained as [28]

$$\hat{r}_k = \frac{-1}{\alpha} \mathcal{I}m\left(\ln\left(\frac{\lambda_k}{|\lambda_k|}\right)\right), \quad k = 1, \ldots, d \qquad (4)$$

where $\mathcal{I}m$ denotes imaginary part, $\{\lambda_k, k = 1, \ldots, d\}$ are the eigenvalues of a diagonal unitary matrix. It relates the measurements from the first subarray with the measurements resulting from the second subarray.

*Estimation of Multiple Circles With Different Centers and Radii:* Usually, an image contains several circles which are possibly not concentric and have different radii (see Fig. 3). To apply the proposed method, the center coordinates for each feature are required. To estimate these coordinates, we generate a signal with constant propagation parameter upon the image left and top sides. More details regarding signal generation upon a linear antenna can be found in [23]. The $l$th signal component, generated from the $l$th row, reads: $z_{\text{lin}}(l) = \sum_{m=1}^{N} I(l,m)\exp(-j\mu m)$, where $\mu$ is the propagation parameter [23]. The nonzero sections of the signals, as seen at the left and top sides of the image (see Fig. 3), indicate the presence of features. Each nonzero section width in the left (respectively, the top) side signal gives the height (respectively, the width) of

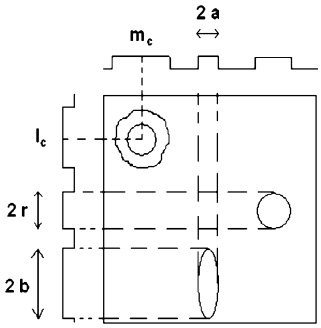


Fig. 3. Model for an image containing several nearly circular or elliptic features. $r$ is the circle radius; $a$ and $b$ are the axial parameters of the ellipse.

the corresponding expected feature. The middle of each nonzero section in the left (respectively, the top) side signal yields an approximate value of the center $l_c$ (respectively, $m_c$) coordinate of each feature. The feature height, width, and center coordinates permit us to select image regions. Each region contains a contour or a set of concentric contours. The proposed method based on circular antenna detects the number of concentric features for each estimated center, in each image region. It yields the values of the fitting circles radii. Then, an optimization method can be used to refine the estimation of each contour. Such a method is applied to the signals generated on our circular antenna is presented in the next section.

*Single Circle Estimation:* Using a circular antenna, a constant parameter propagation scheme yields as well to the radius of a single circle. Signal components are $z(i) = \exp(-j\mu r) + n(i), i = 1, \ldots, S$. The estimated value $\hat{r}$ of $r$ is: $\hat{r} = (1/\mu)\cos^{-1}(\bar{z})$, with $\bar{z} = \mathcal{R}e((1/S)\sum_{i=1}^{S} z(i))$, where $\cos^{-1}$ denotes inverse cosine function and $\mathcal{R}e$ denotes real part. In this algorithm, noise contribution is lowered by averaging. In the next section, we use the fitting circle or ellipse provided by the method presented above to retrieve any distorted contour.

## IV. Optimization Method for the Estimation of Nearly Circular Contours

The optimization methods proposed in [24] and [25] estimate the pixel shift values between a straight line and a nearly linear contour. These methods rely on the assumption that one component of the generated signal is associated with only one unknown pixel shift value in one image row (or column). The proposed circular antenna adapts optimization methods to retrieve distorted star-shaped contours.

### A. Proposed Optimization Method

We employ a circular antenna to retrieve the shift values between an initialization circle and the expected contour. We process successively each quarter of the circle, and retrieve the distortions between one quarter of the initialization circle and the expected contour part that is located in the same quarter of the image. As an example, in Fig. 1, the right bottom quarter of the considered image is represented in Fig. 1(b). An optimization method inspired from [24] is defined as follows:

A contour in the considered subimage is described with a set of polar coordinates by $\{\rho(i), \theta(i), i = 1, \ldots, S\}$. We estimate the $S$ unknowns $\rho(i)$ that characterize the contour, forming a vector

$$\boldsymbol{\rho} = [\rho(1), \rho(2), \ldots, \rho(S)]^T. \tag{5}$$

The basic idea is to consider that $\boldsymbol{\rho}$ can be written as $\boldsymbol{\rho} = [r + \Delta\rho(1), r + \Delta\rho(2), \ldots, r + \Delta\rho(S)]^T$ (see Fig. 1), where $r$ is the radius of a circle that fits the expected contour. The optimization method that we adapt to this problem estimates $\{\Delta\rho(i), i = 1, \ldots, S\}$, that is, the shift values between the initialization circle and the expected contour.

If we take into account the position given by $\boldsymbol{\rho}$ of all edge pixels in (1), the components of signal $\mathbf{z}$ generated out of the image containing the expected contour read

$$z(i) = \exp\left(-j\mu\rho(i)\right), \quad \forall i = 1, \ldots, S. \tag{6}$$

We try to recreate the signal $\mathbf{z}$, whose components are defined by (6), and in which we ignore the $S$ parameters. We start with an initialization vector $\boldsymbol{\rho}_0$, characterizing a quarter of circle that fits the expected distorted contour in the considered subimage. The $S$ components of $\boldsymbol{\rho}_0$ are equal to $r$, the radius value that was previously estimated: $\boldsymbol{\rho}_0 = [r, r, \ldots, r]^T$. Then, with $k$ indexing this recursive algorithm steps, we aim to minimize

$$J(\boldsymbol{\rho}_k) = \left\|\mathbf{z} - \mathbf{z}_{\text{estimated for } \boldsymbol{\rho}_k}\right\|^2 \tag{7}$$

where $\|.\|$ represents the norm induced by the usual scalar product of $\mathbb{C}^S$. The components of $\mathbf{z}_{\text{estimatedfor } \boldsymbol{\rho}_k}$ are defined similarly to the components of $\mathbf{z}$ [see (6)] as a function of the components of $\boldsymbol{\rho}_k$, and the components of $\boldsymbol{\rho}_k$ are obtained from the components of $\boldsymbol{\rho}_0$ by adding a shift: $\boldsymbol{\rho}_k = [r + \Delta\rho_k(1), r + \Delta\rho_k(2), \ldots, r + \Delta\rho_k(S)]^T$. To estimate $\boldsymbol{\rho}$, we use the variable step gradient method. The series vectors are obtained from the relation $\forall k \in \mathbb{N} : \boldsymbol{\rho}_{k+1} = \boldsymbol{\rho}_k - \beta\nabla(J(\boldsymbol{\rho}_k))$, where $\beta$ is the step for the descent. The recurrence loop is

$$\boldsymbol{\rho}_k \rightarrow \mathbf{z}_{\text{estimated for } \boldsymbol{\rho}_k} \rightarrow J(\boldsymbol{\rho}_k). \tag{8}$$

The gradient is estimated using finite differences. When $k$ tends to infinity, the criterion $J$ tends to zero and $\rho_k(i) = r + \Delta\rho(i) = \rho(i), \forall i = 1, \ldots, S$.

We denote by $\widehat{\boldsymbol{\rho}}$ the vector including all the estimated values $\rho_k(i), i = 1, \ldots, S$, with $k$ tending to infinity.

A more elaborated method based on DIRECT algorithm [29] and spline interpolation can be adopted to reach the global minimum of the criterion $J$ of (7). This method is applied to modify recursively the signal $\mathbf{z}_{\text{estimated for } \boldsymbol{\rho}_k}$. At each step of the recursive algorithm, vector $\boldsymbol{\rho}_k$ is computed by interpolating between some "node" values that are retrieved by DIRECT. The main property of DIRECT is that it obtains the global minimum of a function. DIRECT normalizes the research space in a hypercube and evaluates the solution which is located at the center of this hypercube. Then, some solutions are evaluated and the hypercube is divided into smaller cubes, supporting the zones were the evaluations are small. Let $O$ be an integer smaller than $S$. A cubic spline $f$ interpolating on the partition $\{y(1), \ldots, y(O)\}$ of $\{1, \ldots, S\}$ that we call "node points," to the elements $\rho(1), \ldots, \rho(S)$, is a function for which $f(y(k)) =$

$\rho(y(k))$ for $k = 1, \ldots, O$. It is a piecewise polynomial function that consists of $O - 1$ cubic polynomials $f_k$ defined on the ranges $[y(k), y(k+1)]$. Furthermore, each $f_k$ is joined at $y(k)$, for $k = 2, \ldots, O-1$, so that $\rho'(y(k)) = f'(y(k))$ and $\rho''(y(k)) = f''(y(k))$ are continuous. The $k$th polynomial curve, $f_k$, is defined over the fixed interval $[y(k), y(k+1)]$ and is a third order polynomial. Then, the interpolation provides an approximate value of $S$ elements starting from $O$ elements. Spline interpolation permits to obtain a continuous estimated contour, and cubic splines [31] provide an acceptable compromise between computational load and interpolation accuracy. The computational load of DIRECT algorithm grows drastically when the number of sensors, or equivalently the number of unknown phase values, increases. We accelerate DIRECT algorithm by reducing the number of retrieved unknowns. Then, we propose spline interpolation to obtain the $S$ components of $\widehat{\boldsymbol{\rho}}$. We interpolate a subset of values of $\boldsymbol{\rho}_k$, which are retrieved by DIRECT algorithm. The more interpolation nodes, the more precise the estimation, but the slower the algorithm.

### B. Summary of the Proposed Method

The proposed method for distorted contour estimation is summarized as follows.

- Generation of a signal with constant parameter, on a linear antenna placed at the top of and aside the image.
- Estimation of the centers of the circles or ellipses that fit the expected contours.
- Variable speed propagation scheme upon the proposed circular antenna: Estimation of the number of circles by MDL criterion, estimation of the radius of each circle fitting any expected contour [see (1) and (2)] or the axial parameters of the ellipse.
- Estimation of the radial distortions, in a polar system, between any expected contour and the circle or ellipse that fits this contour. Either the gradient method or the combination of DIRECT and spline interpolation may be used to minimize the criterion $J$ of (7).

## V. Results and Discussion

We compare the proposed methods with a least-squares one, Hough transform and GVF. The efficiency of the proposed methods is measured by the mean error $\mathrm{ME}_{\boldsymbol{\rho}}$ over the coordinates of the pixels of the contour. For the four quarters of an image, the coordinates of the pixels of the contour are contained in the vector $\boldsymbol{\rho}$ defined in (5), and their estimates are contained in vector $\widehat{\boldsymbol{\rho}}$. $\mathrm{ME}_{\boldsymbol{\rho}} = (1/S)\sum_{i=1}^{S} |\widehat{\boldsymbol{\rho}}(i) - \boldsymbol{\rho}(i)|$ where $|\cdot|$ means absolute value. The proposed circle fitting method is applied to images having $N = 200$ columns and rows. The number of sensors for each image quarter is $S = 400$, larger than the minimum acceptable value (see Section II-B). The algorithms for center and radius estimation are run using a propagation parameter set at $\alpha = 1.35 \times 10^{-2}$. This optimal value is experimentally defined in [26] for almost the same number of sensors. In [26], a value for the length of each subarray was empirically found to provide optimal results, namely $M = \sqrt{S} = 20$. Other experiments confirmed these values [24], [25]. When a constant parameter signal generation is performed, $\mu = 5 \times 10^{-3}$. This value of $\mu$ avoids phase indetermination [24], [25].

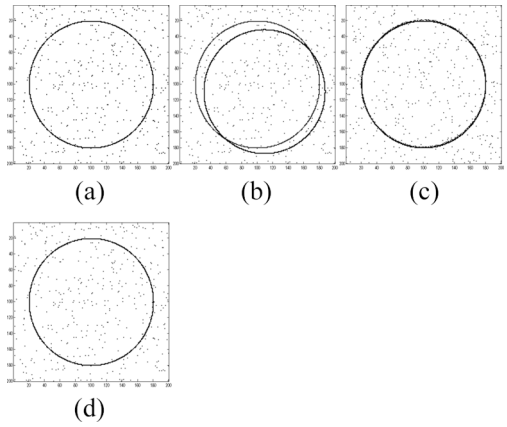


Fig. 4. (a) Processed, (b) superposition processed, and result obtained after applying a least-squares method for circle fitting: $\mathrm{ME}_{\boldsymbol{\rho}} = 4.5$ pixels, (c) superposition processed, and result obtained after applying the Hough transform: $\mathrm{ME}_{\boldsymbol{\rho}} = 0.7$ pixel, (d) superposition processed and result obtained after applying the proposed method: $\mathrm{ME}_{\boldsymbol{\rho}} = 0.3$ pixel.

### A. Hand-Made Images

We first consider the case where one circle is expected in a noisy image. Fig. 4 exemplifies the results obtained with a least-squares fitting method [9], and the proposed circle fitting method.

Center coordinates are (100, 100); the radius value is 80 pixels. When the image is not noisy, there is no bias over the estimated parameters, for all methods. Fig. 4(a) contains 1% of noisy pixels with value 1. We performed 100 trials with the same circle and noise parameters, and different noise realization for each trial. Least-squares fitting [see Fig. 4(b)] provides a 7-pixel bias, and a 9-pixel bias, respectively, over the two center coordinates of the center, and a 1.3 pixel bias over the radius of the circle. Generalized Hough transform, with prior knowledge of the radius, provides center coordinates (100, 100). With the prior knowledge of these center coordinate values, Hough transform, provides a 0.2 pixel bias over the radius value [see Fig. 4(c)]. The proposed method leads to a 0.2 and 0.3 pixel bias over the coordinates of the center, and a 0.2 pixel bias over the radius value [see Fig. 4(d)]. It is more robust to noise than the least-squares method, when a single circle in an impaired image is considered. These results validate the remarks provided in [10], where the sensitivity of least-squares-fit of circle to outliers is underlined.

Fig. 4(c) exemplifies the ability of Hough transform to handle the cases of noisy images. We compared quantitatively and statistically the proposed method with the Hough transform method when a single circle is expected, in a noisy image context. The nonimpaired image contains a circle with radius 80 pixels. We performed 100 trials with different noise realizations, with 2% of noisy pixels in the image, and obtained mean error values over the radius which are, respectively, 1.05 pixels when variable parameter propagation scheme is performed [see (4)]; 1.20 when constant parameter propagation scheme

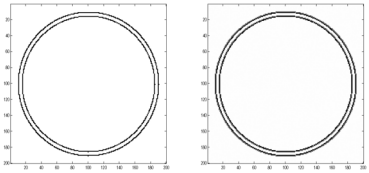


Fig. 5. (a) Processed, (b) result (superimposed), with the proposed method for radius estimation or equivalently with Hough transform or a least-squares fitting method: $\mathrm{ME}_{\boldsymbol{\rho}} = 0.1$ (resp., 0.3 for Hough transform and 0.4 for the least-squares fitting method).

is performed and $\hat{r} = (1/\mu)\cos^{-1}(\bar{z})$; and 1.15 pixels when Hough transform is applied.

Like the proposed method, Hough transform is supposed to retrieve the radius of two close concentric circles. We considered the case of an image containing two concentric circles. The expected radius values are 85 and 90 pixels [see Fig. 5(a)], thus differing by only 6%. When the proposed method is applied, MDL criterion detects two circles, the estimated radius values are 85.1 and 89.9 pixels, and in these conditions the required computational time is 0.359 s on a 3.0-GHz Pentium 4 PC running under Windows. The same computer and software are used throughout all experiments. When Hough transform is run, $\rho$ axis is quantized so that the step between two values is 0.3 pixel, and $\theta$ axis is quantized to $S$ values. Estimated radius values are 84.7 and 90.3 pixels, and the required computational time is 0.51 s. When the least-squares fitting method [11] is used the estimated radius values are 85.4 and 90.3 pixels [see Fig. 5(b)]. The required computational time is 0.95 s.

In the next experiment, we study the sensitivity of the proposed optimization methods to initialization. Gradient algorithm minimizes the criterion of (7). We have been confident that gradient algorithm gives good results for images containing continuous contours and low-valued noise pixels. The descent step parameter is updated at each iteration: initial descent step parameter is $\beta_0 = 0.05$, the step variation is so that $\beta_{k+1} = 1.05\beta_k$. We consider an image impaired with 5% of noisy pixels with value 0.1, containing one circle with center coordinates (100, 100) and radius 80. We choose an initialization circle with center coordinates (70, 70). Hough transform yields, as could be expected, to a biased radius value, more precisely 122.1 pixels. Radius value 20 pixels is used for the initialization. The result circle, obtained after 350 iterations of gradient algorithm, has center coordinates (100, 100) and radius 80: all pixel shifts are canceled. This case is not easily handled by GVF. To converge in a few seconds, the GVF method has to be initialized with a contour which is close to the expected one. Furthermore, the gradient strength has to be set high enough when the edge map of the image is derived [18]. Conversely, the proposed signal generation process transcripts the content of all pixels on one direction $D_i$ (see Fig. 2) and, thus, takes necessarily any feature into account. In the example of Fig. 6(a), we consider a distorted and disrupted contour in a noisy environment. We have been confident that spline interpolation yields a continuous result contour, and that DIRECT handles the case where noisy pixels have the same value as the contour pixels. Fig. 6(b) shows

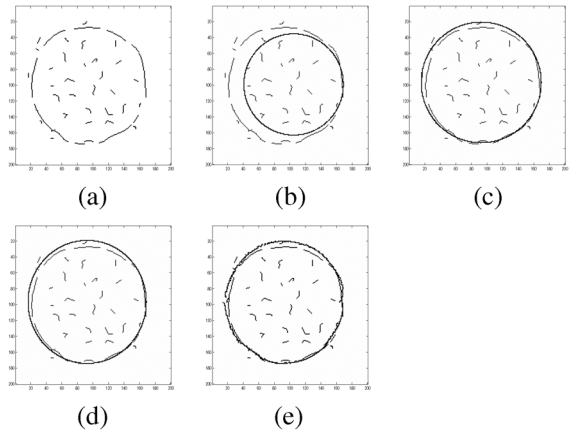


Fig. 6. Biased center and radius estimation, proposed optimization algorithm using DIRECT and spline interpolation. (a) Processed (b) initialization by the least-squares method, (c) initialization by the Hough transform, (d) initialization by the proposed method, (e) superposition processed and final result, $\mathrm{ME}_{\boldsymbol{\rho}} = 0.9$ pixel.

the result obtained with least-squares fitting. Fig. 6(b) shows the result obtained with the Hough transform, used with the center coordinates provided by the proposed method-signal generation upon linear antenna. Fig. 6(d) shows the result obtained with the proposed method for circle fitting. Note that there is a slight bias on the estimation of the center coordinates and the radius. We use this result to initialize the optimization method. Ten iterations of DIRECT are run, with 6 nodes for spline interpolation. Fig. 6(e) shows that in spite of this bias, the proposed optimization method yields a continuous result contour, without focusing on noisy pixels. We now perform a statistical study on the proposed optimization algorithm using variable step gradient method. The proposed optimization method and gradient vector flow [18] are applied to images containing a distorted circle; [19] presents a statistical study on noisy images containing a harmonic shape. A standard GVF method and a generalized version of GVF give satisfactory results when noise percentage values up to 10% are employed. Our goal is to demonstrate the sensitivity of the proposed method compared to GVF, when the considered distortions are no longer harmonic but irregular. Values of the parameters for GVF method [19] are the following. For the computation of the edge map: 100 iterations; $\mu_{\mathrm{GVF}} = 0.09$ (regularization coefficient); for the snakes deformation: 100 initialization points and 50 iterations; $\alpha_{\mathrm{GVF}} = 0.2$ (tension); $\beta_{\mathrm{GVF}} = 0.03$ (rigidity); $\gamma_{\mathrm{GVF}} = 1$ (regularization coefficient); $\kappa_{\mathrm{GVF}} = 0.8$ (gradient strength coefficient). We study the robustness of the proposed method and GVF to both noise impairment and curvature. Statistical results presented below are obtained with 15 images containing a different distorted circle, with variable distortion amplitude. The maximum distortion amplitude and the standard deviation of the distortions is different for each image. The least and most distorted contours are drawn in Fig. 7(a) and (b), respectively. Fig. 7 also presents the results obtained with the proposed method. Random noise is added to various percentage values of the image pixels: 0%, 1%, 2%, 4%, 6%, and 8%.

The original non-noisy images have pixel values 1 (expected contour) or 0 (background). They are impaired with Gaussian

TABLE I
ME VALUES (IN PIXELS) OBTAINED WITH THE PROPOSED METHOD (A) AND WITH GVF (B), VERSUS DISTORTION (MAXIMUM AMPLITUDE; STANDARD DEVIATION) AND NOISE PERCENTAGE

| | $ME$ values (pixels) | | | | | | | | | | | | | |
|---|---|---|---|---|---|---|---|---|---|---|---|---|---|---|
| noise / distortion | 0% | | 1% | | 2% | | 4% | | 6% | | 8% | | Mean value $ME_d$ | |
| | (A) | (B) | (A) | (B) | (A) | (B) | (A) | (B) | (A) | (B) | (A) | (B) | (A) | (B) |
| (9.28; 1.66) | 1.44 | 1.40 | 1.83 | 1.42 | 2.00 | 1.43 | 2.05 | 1.44 | 2.08 | 1.45 | 2.10 | 1.47 | 1.91 | 1.43 |
| (11.84; 1.97) | 1.51 | 1.62 | 1.96 | 1.64 | 2.06 | 1.66 | 2.07 | 1.68 | 2.12 | 1.69 | 2.23 | 1.70 | 1.99 | 1.66 |
| (14.68; 2.42) | 1.68 | 1.67 | 1.98 | 1.69 | 2.09 | 1.72 | 2.10 | 1.72 | 2.16 | 1.73 | 2.27 | 1.74 | 2.04 | 1.71 |
| (17.76; 2.93) | 1.70 | 1.78 | 2.00 | 1.85 | 2.11 | 1.86 | 2.12 | 1.87 | 2.18 | 1.88 | 2.28 | 1.89 | 2.06 | 1.85 |
| (18.36; 3.46) | 1.72 | 2.07 | 2.02 | 2.08 | 2.13 | 2.08 | 2.14 | 2.08 | 2.19 | 2.11 | 2.30 | 2.12 | 2.08 | 2.09 |
| (21.05; 3.07) | 1.81 | 2.10 | 2.17 | 2.10 | 2.24 | 2.10 | 2.25 | 2.11 | 2.26 | 2.12 | 2.32 | 2.15 | 2.17 | 2.11 |
| (21.55; 3.62) | 1.82 | 2.28 | 2.18 | 2.29 | 2.26 | 2.31 | 2.27 | 2.32 | 2.32 | 2.33 | 2.38 | 2.34 | 2.20 | 2.31 |
| (24.88; 4.25) | 1.84 | 2.59 | 2.19 | 2.61 | 2.30 | 2.62 | 2.32 | 2.63 | 2.55 | 2.64 | 2.56 | 2.65 | 2.29 | 2.62 |
| (28.34; 5.01) | 2.02 | 2.69 | 2.29 | 2.71 | 2.46 | 2.72 | 2.67 | 2.74 | 2.77 | 2.75 | 2.79 | 2.76 | 2.50 | 2.72 |
| (31.85; 5.21) | 2.18 | 3.04 | 2.37 | 3.11 | 2.52 | 3.12 | 2.85 | 3.14 | 2.89 | 3.18 | 2.90 | 3.19 | 2.61 | 3.13 |
| (35.39; 5.86) | 2.19 | 3.12 | 2.47 | 3.16 | 2.60 | 3.19 | 2.89 | 3.21 | 2.90 | 3.34 | 2.96 | 3.41 | 2.66 | 3.23 |
| (38.90; 6.61) | 2.30 | 3.43 | 2.51 | 3.51 | 2.62 | 3.55 | 2.95 | 3.59 | 3.00 | 3.61 | 3.01 | 3.62 | 2.73 | 3.55 |
| (42.33; 7.42) | 2.42 | 3.69 | 2.63 | 3.71 | 2.67 | 3.82 | 3.00 | 3.83 | 3.13 | 3.84 | 3.19 | 3.85 | 2.84 | 3.79 |
| (45.63; 8.28) | 2.43 | 4.05 | 2.89 | 4.06 | 2.96 | 4.07 | 3.14 | 4.08 | 3.20 | 4.09 | 3.34 | 4.09 | 2.99 | 4.07 |
| (48.75; 9.22) | 2.77 | 4.21 | 3.11 | 4.22 | 3.16 | 4.23 | 3.30 | 4.27 | 3.38 | 4.28 | 3.43 | 4.33 | 3.19 | 4.25 |
| Mean value $ME_n$ | 1.98 | 2.64 | 2.30 | 2.67 | 2.41 | 2.69 | 2.54 | 2.71 | 2.60 | 2.73 | 2.67 | 2.75 | 2.41 | 2.69 |

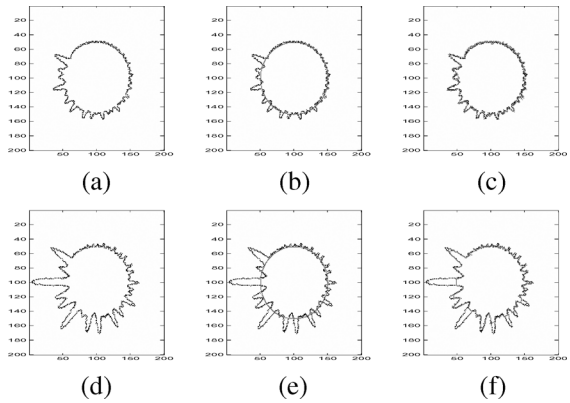


Fig. 7. Examples of processed images containing (a) the least and (d) the most distorted circles; (b), (e) initialization; and (c), (f) estimation using the proposed method. $\mathrm{ME}_{\boldsymbol{\rho}} = 1.4$ pixel and 2.7 pixel.

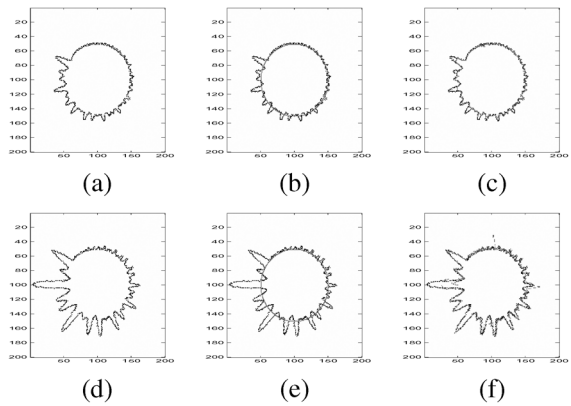


Fig. 8. Examples of processed images containing (a) the least and (d) the most distorted circles; (b), (e) initialization; and (c), (f) estimation using GVF algorithm. $\mathrm{ME}_{\boldsymbol{\rho}} = 1.4$ pixel and 4.1 pixels.

noise having mean $m_{No}$ and standard deviation $\sigma_{No}$ equal, respectively, to 20% and 1% of the value of a pixel that belongs to the expected contour. For each image quarter, computational times are, respectively, 0.28 s for signal generation, 0.15 s for running variable step gradient algorithm $-50$ iterations are performed, and 12 s for running GVF algorithm. Furthermore, the proposed method is five times faster than GVF. For each noise percentage and each contour, 100 trials are performed, with a different noise realization for each trial. To assess the performance of the proposed method, we define the mean error ME

$\mathrm{ME} = (1/100)\sum_{j=1}^{100} ME_{\boldsymbol{\rho}_j}$, where $j$ indexes the trials and $\mathrm{ME}_{\boldsymbol{\rho}_j}$ is the mean error over all pixels of the contour, obtained at the $j$th trial.

Table I presents the ME values for all maximum distortion amplitude and noise percentage values. Table I presents the ME values for all images and noise percentage values. The first column of Table I indicates the couple (maximum distortion amplitude; standard deviation of the distortions), for all images. Table I shows that mean error values are between 1.44 and 3.43 pixels for the proposed method and between 1.40 and 4.33 pixels for GVF. The mean values $\mathrm{ME}_d$ of the ME values obtained for each distortion amplitude demonstrate that GVF is limited by high curvature values. These mean values increase rapidly when the maximum distortion amplitude increases. The mean values $\mathrm{ME}_n$ of the ME values obtained for each noise percentage highlight that the proposed method outperforms GVF for all chosen noise percentage values. The errors obtained with GVF are the consequence of its inability to progress into the furthest sections of some concavities, while the proposed method retrieves the pixel shifts whatever their values are. The increase in pixel bias come from unexpected fluctuations: noise corrupts the phase of the generated signals.

*Multiple Circles With Different Centers and Radii:* We retrieve nearly circular features which may be concentric or not, and which have different radii. GHT handles the case of nonconcentric circles with same radius: it provides a good estimation of each circle center, when the radius of the expected circles is known. We use the proposed method for the characterization of several contours (see Section III). We perform constant parameter propagation scheme. Starting from the estimation of the center of each feature, the method proposed in Section III estimates the number of concentric features and the approximate radius value of each feature.

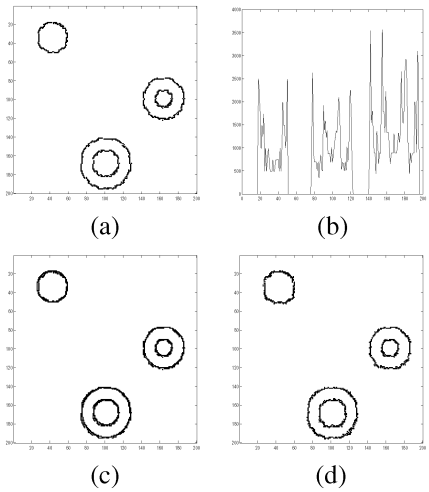


Fig. 9. Multiple circles: (a) processed (b) signal generated upon the left side of the image (c) initialization (d) result with gradient method.

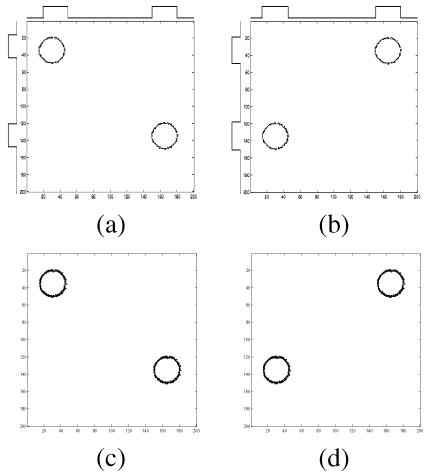


Fig. 10. Two circles with different centers and same radius. (a), (b) Processed images, modulus of the generated signals. (c), (d) Superposition processed and result with gradient method.

Fig. 9(a)–(d) shows an image with multiple circles, the signal generated upon the left side of the image, the initialization and the final result obtained by the proposed methods. Starting from the modulus of the generated signal, we apply hard threshold. Then we take the derivative of the binary signal obtained. The points with nonzero derivative indicate successively the beginning and end of each nonzero section of generated signal. All circles in the image have different radius, and the proposed method retrieves efficiently the number of concentric circles -through MDL criterion- and the parameters of all circles. Distortions are retrieved by the proposed optimization method. In spite of a bias (3, 2) pixels over estimation of the two center coordinates of the bottom circles couple, the proposed optimization method retrieves the expected circles.

*Two Circles With Different Centers and Same Radius:* We consider the ambiguous case where an image contains two circles with center coordinates $(l_{c1}, m_{c1})$ and $(l_{c2}, m_{c2})$, and same radius $r$. Exchanging either horizontal or vertical coordinates of the centers does not change the modulus of the generated signals. The phase of the generated signals overcomes this ambiguity. The signal component at row $l_{ci}$, $i = 1, 2$ indexing circles 1 and 2 (see Fig. 1), reads $z_{\text{lin}}(l_{ci}) = \sum_{m=1}^{N} I(l,m)\exp(-j\mu m) = e^{-j\mu(m_{ci}-r)} + e^{-j\mu(m_{ci}+r)} = z_{\text{lin}}(l_{ci}) = 2e^{-j\mu m_{ci}}\cos(\mu r)$. Therefore, the center horizontal coordinate is obtained by

$$m_{ci} = \frac{-1}{\mu}\mathcal{I}m\left(\ln\left(\frac{z_{\text{lin}}(l_{ci})}{2\cos(\mu r)}\right)\right), \quad i = 1, 2. \tag{9}$$

We consider images of Fig. 10, where circle radius is 15 pixels. Circles are only slightly distorted, which leads to the same length for all signal nonzero sections. For the first (respectively, second) processed image [see Fig. 10(a) and (b)], the first circle center coordinates are $(l_{c1}, m_{c1}) = (30, 35)$, the second circle center coordinates are $(l_{c2}, m_{c2}) = (135, 165)$ [respectively, (30,165) and (135,35) for the second image]. For both images, the estimation obtained from the modulus of the generated signals (see aside and on top of the each image in Fig. 10) are, for the horizontal coordinates: 165, 35; for the vertical coordinates: 135, 30. The phase of the generated signals associates the horizontal coordinates obtained from the signal modulus, with the vertical coordinates, obtained from the phase [see (9)]: $l_{c1} = 30$ pixels yields $m_{c1} = 35.1$ (respectively, 165.2 for the second image), and $l_{c2} = 135$ pixels yields $m_{c2} = 35.1$. Thus, each circle is retrieved. Thus, by studying the phase of the generated signals, we distinguish between the first image and second one. Running the proposed optimization method yields the results of Fig. 10(c) and (d).

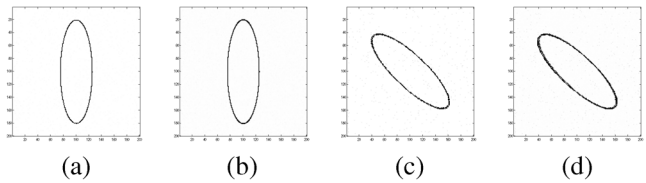


Fig. 11. Ellipse (and, respectively, rotated ellipse) fitting: (a), (c) processed; (b), (d) superposition processed and result obtained after applying the proposed method for ellipse fitting: $\text{ME}_{\boldsymbol{\rho}} = 0.7$ (respectively, $\text{ME}_{\boldsymbol{\rho}} = 0.6$) pixel.

*Rotated Ellipse Retrieval:* Let us consider the case of a vertical ellipse or a rotated ellipse [see Fig. 11(a) and (c)]. An ellipse is characterized by two axial parameters instead of a constant radius. For the case where an ellipse is expected, the method proposed in [22] leads to two axial parameters and the ellipse center. The axes of the ellipse may not be horizontal and vertical [see Fig. 11(c)]. In this case, we propose the following procedure. We consider the signals generated on the linear antenna placed at the top and the left side, and more precisely the nonzero section length of the signals. The image is rotated until these lengths are the most different from each other. The ellipse of Fig. 11(c) has center coordinates (100, 100), and axial parameters 80 and 25 pixels. Its inclination is 47°. We perform rotations of the image containing the ellipse, with a 1° step between each rotation, and test the length of the nonzero sections of the generated signals after each rotation. The estimated value of the ellipse inclination is 47° and the corresponding estimated axial parameter values are 80 and 25 pixels. When the ellipse is distorted, the proposed optimization method is logically applied.

### B. Real-World Images

The proposed methods summarized in Section IV-B are applied on real-world images [see Fig. 12(1a)–(3a)]. Real-world images are supposed to be more difficult to process than hand-made ones. This is due to the disruptions in the expected contours. Therefore, we use the combination of the robust DIRECT method and spline interpolation to estimate distortions. First, we compute the mean of the image three color components. We apply a Canny edge-enhancing operator. The expected contours are supposed to be centered in the middle of the image. The centers of the initialization circles are taken as the center of the image, that is, pixel (100, 100). The initialization circles number and radius are obtained as follows. We apply variable speed propagation scheme on the proposed circular antenna. Then TLS-ESPRIT method yields the radius values. MDL criterion provides the number of expected nearly circular contours. Together, DIRECT combined with spline interpolation are fast enough to be compared with gradient vector flow, if a small number of nodes is chosen for the interpolation. The first processed image concerns pie calibration. Fig. 12(1a) gives the original color image. Fig. 12(1b) gives the result of Canny edge enhancement, Fig. 12(1c) gives the initialization circle superimposed to the processed image. Fig. 12(1d) shows that gradient provides a contour which is not continuous and whose pixels go aside the pixels of the expected contour. When gradient method is employed the mean error value $ME_{\boldsymbol{\rho}}$ is 2.0 pixels. Fig. 12(1e) gives the result using GVF. Mean error value $ME_{\boldsymbol{\rho}}$ is 1.6 pixels. Fig. 12(1f) gives the result obtained by DIRECT combined with spline interpolation. When this robust optimization method is used, the mean error value $ME_{\boldsymbol{\rho}}$ is 0.6 pixel. Parameters used to run DIRECT and spline interpolation are six interpolation nodes and five iterations for DIRECT. For this image the required computational time is 26 s. Then we consider biometrics [iris fitting, see Fig. 12(2)] and checking mechanical tool size [see Fig. 12(3)].

Table II gives the mean error values $ME_{\boldsymbol{\rho}}$, for all images. It shows that for all images, DIRECT combined with spline interpolation gives the best result in terms of mean error.

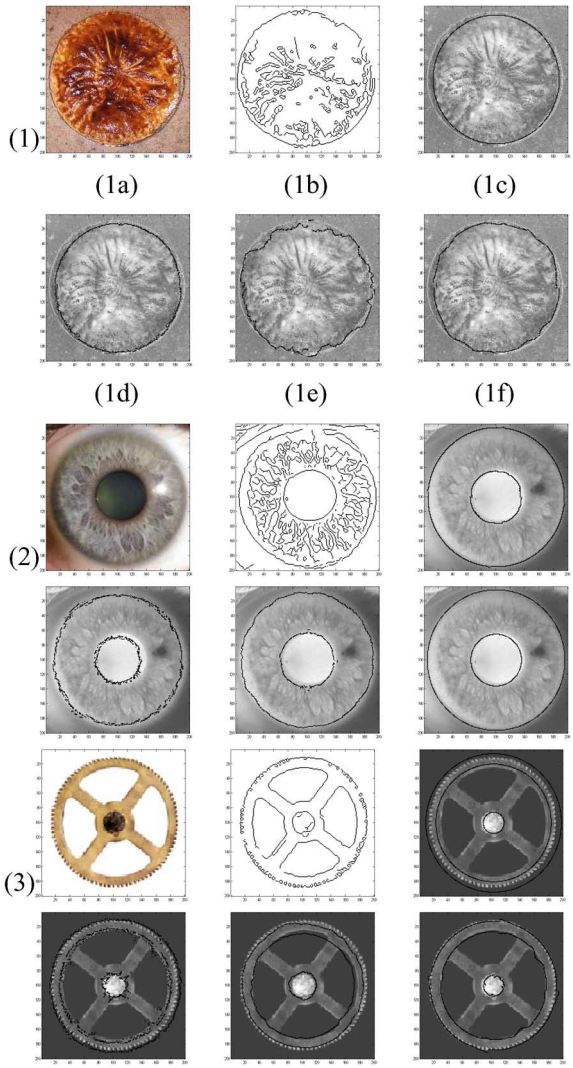


Fig. 12. (1a)–(3a) Processed image; (1b)–(3b) result of Canny operator; (1c)–(3c) initialization; (1d)–(3d) result obtained with gradient method; (1e)–(3e) result obtained with GVF; (1f)–(3f) result obtained with DIRECT combined with spline interpolation.

TABLE II
REAL-WORLD IMAGES: ME VALUES (IN PIXELS)

| image | (1) | (2) | (3) |
|---|---|---|---|
| Gradient: $ME_{\rho}$ | 0.9 | 0.8 | 0.5 |
| GVF: $ME_{\rho}$ | 1.8 | 0.7 | 0.5 |
| DIRECT, spline: $ME_{\rho}$ | 0.8 | 0.4 | 0.2 |

## VI. CONCLUSION

This paper investigates the estimation of distorted circular contours in images by means of array processing and optimization methods. We demonstrate the effectiveness and efficiency of a circular antenna for the generation of linear phase signals out of images containing circular contours. This enables the use of high-resolution methods and optimization algorithms in the estimation of distorted circles in images. A variable speed propagation scheme and MDL criterion estimate the number and radii of concentric circles. Using a circular antenna, a constant parameter propagation scheme and optimization methods extend circle estimation to nearly circular star-shaped contour retrieval. Gradient algorithm, or DIRECT algorithm combined with spline interpolation, retrieve the pixel shifts between an initialization circle and the expected contour. We generalize the procedure to the estimation of multiple circles with different centers and radii, and rotated ellipses. We applied the proposed methods to hand-made and real-world images and compared the results obtained with those from least-squares fitting, Hough transform and gradient vector flow. The retrieval of one circle in a noisy image exemplified the robustness to noise of our approach. By considering concentric circles, we proved the ability of our approach to distinguish between two close concentric circles. With an experiment concerning a disrupted contour in a noisy image, we showed that DIRECT combined with spline interpolation yields a continuous result in difficult conditions. The proposed signal generation and our optimization method using gradient outperforms gradient vector flow when contours with high curvature are retrieved. The generalization of our approach to multiple non concentric contours and ellipses was illustrated. The robust optimization method that combines DIRECT with

spline interpolation was successfully applied to real-world images and compared with gradient vector flow, leading to low pixel bias. The results of the experiments show that the proposed method is fast and promising for feature retrieval. Further work could consist in retrieving occluded circles and ellipses.

## ACKNOWLEDGMENT

The authors would like to thank the anonymous reviewers for their careful reading and their fruitful remarks, which have contributed in improving the quality of the paper.

## REFERENCES

[1] U. M. Landau, "Estimation of a circular arc center and its radius," *Comput. Vis. Graph. Image Process.*, no. 38, pp. 317–326, Jun. 1986.
[2] J. F. Crawford, "A noniterative method for fitting circular arcs to measured points," *Nucl. Instrum. Meth. Phys. Res.*, no. 211, pp. 223–225, 1983.
[3] V. Karimäki, "Effective circle fitting for particle trajectories," *Nucl. Instrum. Meth. Phys. Res.*, no. 305, pp. 187–191, 1991.
[4] I. Kasa, "A circle fitting procedure and its error analysis," *IEEE Trans. Instrum. Meas.*, vol. IM-25, no. 1, pp. 8–14, Mar. 1976.
[5] G. Coath and P. Musumeci, "Adaptive arc fitting for ball detection in robocup," in *Proc. APRS Workshop on DIC*, Brisbane, Australia, Feb. 2003, pp. 63–68.
[6] S. D. Connell and A. K. Jain, "Template-based online character recognition," *Pattern Recognit.*, vol. 34, no. 1, pp. 1–14, 2001.
[7] M. A. T. Figueiredo and A. K. Jain, "Unsupervised learning of finite mixture models," *IEEE Trans. Pattern Anal. Mach. Intell.*, vol. 24, no. 3, pp. 381–396, Mar. 2002.
[8] N. Ayache and O. D. Faugeras, "HYPER: A new approach for the recognition and positionning of two-dimensionnal objects," *IEEE Trans. Pattern Anal. Mach. Intell.*, vol. 8, no. 1, pp. 44–54, Jan. 1986.
[9] W. Gander, G. H. Golub, and R. Strebel, "Least-squares fitting of circles and ellipses," *BIT*, no. 34, pp. 558–578, 1994.
[10] J. Borkowski, B. J. Matuszewski, J. Mroczka, and L.-K. Shark, "Geometric matching of circular features by least-squares fitting," *Pattern Recognit. Lett.*, no. 23, pp. 885–894, 2001.
[11] P. O'Leary, M. Harker, and P. Zsombor-Murray, "Direct and least-squares fitting of coupled geometric objects for metric vision," *Proc. Inst. Elect. Eng.*, vol. 152, no. 6, pp. 687–694, Dec. 2005.
[12] Y. J. Ahn and H. O. Kim, "Approximation of circular arcs by Bézier curves," *J. Comput. Appl. Math.*, no. 81, pp. 145–163, 1997.
[13] Y. J. Ahn, Y. S. Kim, and Y. Shin, "Approximation of circular arcs and of a set curves by Bézier curves of high degree," *J. Comput. Appl. Math.*, no. 167, pp. 405–416, 2004.
[14] J. Illingworth and J. Kittler, "A survey of the Hough transform," *Comput. Vis. Graph. Image Process.*, no. 44, p. 87116, 1988.
[15] D. H. Ballard, "Generalizing the Hough transform to detect arbitrary shapes," *Pattern Recognit.*, vol. 13, no. 2, pp. 111–122, 1981.
[16] C. L. Tisse, L. Martin, L. Torres, and M. Robert, "Person identification technique using human iris recognition," in *Proc. Int. Conf. Vision interface*, May 2002, pp. 294–299.
[17] M. Kass, A. Witkin, and D. Terzopoulos, "Snakes: Active contour model," *Int. J. Comput. Vis.*, pp. 321–331, 1988.
[18] C. Xu and J. L. Prince, "Gradient vector flow: A new external force for snakes," in *Proc. IEEE Comput. Soc. Conf. Computer Vision, Pattern Recognition*, Jun. 1997, pp. 66–71.
[19] X. Xianghua and M. Mirmehdi, "RAGS: Region-aided geometric snake," *IEEE Trans. Image Process.*, vol. 13, no. 5, pp. 640–652, May 2004.
[20] J. F. Aujol, G. Aubert, and L. Blanc-Féraud, "Wavelet-based level set evolution for classification of textured images," *IEEE Trans. Image Process.*, vol. 12, no. 12, pp. 1634–1641, Dec. 2003.
[21] K. Imen, R. Fablet, J.-M. Boucher, and J.-M. Augustin, "Region-based segmentation using texture statistics and level-set methods," in *Proc. IEEE ICASSP*, Apr. 2006, no. 2, pp. 693–696.
[22] H. K. Aghajan, "Subspace Techniques for image understanding and computer vision," Ph.D. dissertation, Stanford Univ., Stanford, CA, 1995.
[23] H. K. Aghajan and T. Kailath, "Sensor array processing techniques for super resolution multi-line-fitting and straight edge detection," *IEEE Trans. Image Process.*, vol. 2, no. 4, pp. 454–465, Oct. 1993.
[24] S. Bourennane and J. Marot, "Contour estimation by array processing methods," *Appl. Signal Process.*, 2006, article ID 95634, 15 pages.
[25] S. Bourennane and J. Marot, "Optimization and interpolation for distorted contour estimation," in *Proc. IEEE ICASSP*, Apr. 2006, no. 2, pp. 717–720.
[26] H. Aghajan and T. Kailath, "SLIDE: Subspace-based line detection," *IEEE Trans. Pattern Anal. Mach. Intell.*, vol. 16, no. 11, pp. 1057–1073, Nov. 1994.
[27] M. Wax and T. Kailath, "Detection of signals information theoretic criteria," *IEEE Trans. Acoust., Speech, Signal Process.*, vol. ASSP-33, no. 2, pp. 387–392, Apr. 1985.
[28] R. Roy and T. Kailath, "ESPRIT: Estimation of signal parameters via rotational invariance techniques," *IEEE Trans. Acoust., Speech, Signal Process.*, vol. 37, no. 7, pp. 984–995, Jul. 1989.
[29] D. R. Jones, C. D. Pertunen, and B. E. Stuckman, "Lipschitzian optimization without the Lipschitz constant," *J. Optim. Appl.*, vol. 79, no. 157-81, 1993.
[30] H. K. Aghajan, B. H. Khalaj, and T. Kailath, "Estimation of multiple 2-D uniform motions by SLIDE: Subspace-based line detection," *IEEE Trans. Image Process.*, vol. 8, no. 4, pp. 517–526, Apr. 1999.
[31] G. Wolberg and I. Alfy, "Monotonic cubic spline interpolation," in *Proc. Int. Conf. Computer Graphics*, 1999, pp. 188–195.

**Julien Marot** received the physics engineering diploma from ENSP Marseille, France, in 2003, and the M.Sc. degree in image processing in 2004. He is currently pursuing the Ph.D. degree in the multidimensional signal processing group (GSM), Fresnel Institute (CNRS UMR-6133), Marseille

His research interests include applied image processing and signal processing.

**Salah Bourennane** received the Ph.D. degree from the Institut National Polytechnique de Grenoble, France, in 1990.

Currently, he is a Full Professor at the Ecole Centrale de Marseille, France. His research interests are in statistical signal processing, array processing, image processing, multidimensional signal processing, and performance analysis.